

## Research Article

# Moisture Sorption Behavior and Effects of Temperature, Slice Thickness, and Loading Density on Drying Kinetics of a Local Sweet Potato Cultivar Grown in Bangladesh

Mirza Sahria Kamal <sup>1</sup>, Md Shakil <sup>2</sup>, Tanjina Akter <sup>2</sup>, Sabina Yasmin <sup>3</sup>, Abu Saeid <sup>4</sup>,  
and Mayeen Uddin Khandaker <sup>5,6</sup>

<sup>1</sup>Department of Food Technology and Rural Industries, Bangladesh Agricultural University, Mymensingh 2202, Bangladesh

<sup>2</sup>Department of Food Technology, Chulalongkorn University, Pathumwan, Bangkok 10330, Thailand

<sup>3</sup>Department of Food Engineering and Technology, Hajee Mohammad Danesh Science and Technology University, Dinajpur 5200, Bangladesh

<sup>4</sup>Department of Nutrition and Food Engineering, Daffodil International University, Daffodil Smart City (DSC), Birulia, Savar, Dhaka 1216, Bangladesh

<sup>5</sup>Centre for Applied Physics and Radiation Technologies, School of Engineering and Technology, Sunway University, 47500 Bandar Sunway, Selangor, Malaysia

<sup>6</sup>Department of General Educational Development, Faculty of Science and Information Technology, Daffodil International University, DIU Rd, Dhaka 1341, Bangladesh

Correspondence should be addressed to Mayeen Uddin Khandaker; mayeenk@diu.edu.bd

Received 1 January 2023; Revised 25 May 2023; Accepted 31 May 2023; Published 21 June 2023

Academic Editor: Yogesh Kumar

Copyright © 2023 Mirza Sahria Kamal et al. This is an open access article distributed under the Creative Commons Attribution License, which permits unrestricted use, distribution, and reproduction in any medium, provided the original work is properly cited.

This study is aimed at investigating the moisture sorption behavior and thin-layer drying kinetics of local sweet potato sada (LSPS) variety slices. The sweet potato tubers were sliced at 3, 5, and 7 mm and dried at temperatures of 45, 55, and 62°C at a constant air velocity of 0.6 m/sec in a laboratory-scale cabinet dryer. The BET (Brunauer, Emmet, and Teller) and GAB (Guggenheim-Anderson-De Bore) models were applied to fit the sorption data. Fick's diffusion equation was used to calculate the drying rate constant and effective moisture diffusivity. Our current result reveals that LSPS exhibited an isotherm with a sigmoid (type II) shape, and the GAB model was more goodness of fit than the BET model to clarify the adsorption isotherm of LSPS. The drying time increased with increasing slice thickness but reduced with increasing drying temperature. The drying rate constant for thin-layer drying decreased with an increase in slice thickness but increased with increasing drying temperature. The loading density with two different shapes (French cut and cube cut) also affected the drying rate constant, which decreased with the increase in loading density. Using statistical parameters, five thin-layer drying models were applied to fit the drying data. The findings indicated that the logarithmic model for 45–55°C and the Page model for 62°C were the most suitable models for explaining the drying behavior of LSPS slices. The effective moisture diffusivity increased with increasing slice thickness and drying temperature, ranging from  $7.10 \times 10^{-11}$  to  $1.55 \times 10^{-10}$  m<sup>2</sup>/s over the temperature range studied. The activation energy also increased with increasing slice thickness, and the values were 5.55 and 7.39 kJ/mol for 3 and 5 mm slices, respectively. The findings suggested that slice thickness, drying temperature, and sample loading density on cabinet dryer trays affect the drying kinetics of sweet potato slices.

## 1. Introduction

Sweet potato (*Ipomoea batatas* Lam.) belongs to the family Convolvulaceae commonly known as “Misti Alu” in Bangladesh. It is an essential starch-rich root crop cultivated in more than 100 countries in tropical and subtropical climates [1]. Many nations throughout the world, including South Africa and China, consume sweet potatoes as a staple diet after rice and wheat [2]. China is the world’s largest sweet potato market, with a market share of approximately 65%, followed by Africa, with a share of nearly 19% [3]. About 88.9 million metric tons of sweet potatoes was produced worldwide in 2021, with an increase of around 130 thousand metric tons from the preceding year [4]. In 2019, Bangladesh produced 245,719 metric tons of sweet potatoes, making it the fourth most important crop in the country after rice, wheat, and potatoes [5]. They are an essential source of nutrition in many African countries and play a crucial role in the battle against hunger and food insecurity, which encompasses issues like obesity and overweight [6].

Sweet potatoes are one of the best sources of carbohydrates, dietary fiber, potassium, and vitamin C. In addition, they are low in fat and a rich source of beta-carotene, a precursor to vitamin A, and polyphenols, the least expensive antioxidant source for human health in developing nations [6]. However, sweet potato tubers swiftly degrade after being harvested due to physiological changes and mechanical damage that happened during harvesting, transportation, and handling [7]. Because of their substantial moisture content, freshly harvested sweet potatoes exhibit a high degree of perishability [8].

Drying is one of the traditional methods for preserving and improving agricultural products’ storage quality. The drying process uses heat and mass transfer to get the moisture content down to a safe level. As a result, enzymatic and microbiological activities that cause the degradation of food products are significantly reduced, giving the products a longer shelf life and a lighter weight for storage [9]. Bangladesh has a long history of drying goods under direct sunlight exposure, which is dependent on the climate and can lead to contamination from microbes and other sources [10]. The final product may be damaged by contamination from insects, dust, or deterioration driven on by humid conditions while drying [11]. Agricultural products are now dried mechanically, utilizing the convective approach to combat this situation. Cabinet dryers, among other mechanical dryers, are an inexpensive alternative to dry various agricultural commodities with shortened drying times and increased final product quality [12]. Drying causes an accumulation of sugars, which minimizes the dried product’s water activity ( $a_w$ ), resulting in a very extended shelf life due to inhibiting microbiological growth [13]. Nevertheless, the exceedingly low moisture content of dried products makes them susceptible to moisture absorption, which is linked to rancidity during storage. The moisture sorption isotherm is helpful for anticipating the quality attributes and establishing the operational processing parameters for dried foods. Several works have characterized the sorption isotherms of dried products [14–18].

Numerous studies reported the characteristics of fruits and vegetables using low-cost cabinet drying methods. Some of the notable studies include the common foodstuff such as bitter melon [19], carrot [20], bananas [21], and pumpkin [11]. In these studies, the authors reported that the drying conditions (drying temperature) and sample geometry (slice thickness and shape) affect the drying kinetics and quality of the dried product. To our best knowledge, a few studies investigated the drying kinetics of sweet potato slices. Dinrifo [7] observed the thin drying kinetics of pretreated (blanched in hot water at 100°C and dipped in sodium metabisulfite) sweet potato slices (4 mm) at the temperature of 50, 60, 70, and 80°C using a hot air convective dryer. Olawale and Omole [22] studied the kinetics of thin-layer drying of sweet potato (with three dimensions of 10 × 10 × 5 mm, 20 × 20 × 10 mm, and 20 × 20 × 5 mm) with and without pretreatment at temperatures between 50°C and 80°C in a tray dryer. Doymaz [23] investigated the effect of blanching (hot water blanched at 70°C for 2 min) and drying temperatures (50, 60, and 70°C) on the thin-layer drying characteristics in a cabinet dryer and rehydration ratio of sweet potato slices of 30 × 48 × 5 mm. Oh et al. [14] compared the moisture sorption properties and quality characteristics of dried sweet potato slices (cubic shape of 25 × 25 × 6 mm) of three varieties. The samples were prepared by hot air semidrying at 60°C in a hot air dryer and followed by hot pressing at 180°C for 3 s using a lab-assembled ohmic-heat presser. They reported that the GAB equation was the best model to explain the moisture isotherm properties of dried sweet potatoes based on the mathematical models. Singh and Pandey [24] studied the effect of air temperature (50, 60, 70, 80, and 90°C), velocity (1.5, 2.5, 3.5, 4.5, and 5.5 m/s), and slice thickness (cubes of 5, 8, and 12 mm thick) of sweet potato slices in a cabinet dryer. According to their findings, drying occurred during the falling rate period, and the modified Page model best described the drying behavior of sweet potatoes. None of them studied, to our best knowledge, the effect of sample loading (single, double, and triple layers) and sample shape (cube and French cut) on the drying rate constant and drying rate of sweet potato. Additionally, only a handful of research has examined the moisture sorption behavior of sweet potatoes, despite the fact that it is a helpful tool for predicting and determining the qualities of dried foods and establishing the operating conditions for their processing.

Therefore, our study was designed to investigate (a) the moisture sorption behavior of dried sweet potato with the prediction of moisture adsorption by BET and GAB models; (b) the drying kinetics of sweet potato with varying drying temperatures, thickness, and loading density in a cabinet tray dryer, which is mostly used for drying of fruits and vegetables in Bangladesh; and (c) the effective moisture diffusivity and activation energy for LSPS slices.

## 2. Materials and Methods

**2.1. Sample Collection and Preparation.** The local sweet potato sada (LSPS), which was uniform in size and shape as well as pest- and damage-free, was collected immediately after harvesting from the Mymensingh district of Bangladesh. The

collected samples were immediately transferred to the laboratory and stored in a refrigerator at 4°C until use. The sweet potatoes were cleaned with running tap water for 2-3 min, peeled, and sliced manually. The thickness of potato slices was kept at 3, 5, and 7 mm.

**2.2. Moisture Sorption Behavior.** The moisture sorption characteristics of dried sweet potato were studied in vacuum desiccators at room temperature (30°C) under varying relative humidity (11-93% RH) conditions using nine saturated salt solutions. The saturated salt solutions were prepared using LiCl,  $K_2H_3O_2$ ,  $MgCl_2 \cdot 6H_2O$ ,  $K_2CO_3$ ,  $Mg(NO_3)_2 \cdot 6H_2O$ ,  $CaCl_2$ , NaCl, KCl, and  $KNO_3$ . An accurately weighed 3 g vacuum-dried crushed sample was placed in desiccators with crucibles, and defined relative humidity was maintained using the saturated salt solutions. A pump externally evacuated the desiccators to less than 50 torr. Sample weights were recorded up until they attained a consistent weight. The equilibrium moisture content of the samples was then estimated. To determine the monolayer moisture content for the moisture adsorption process, linear regression was performed with the BET (Brunauer, Emmet, and Teller) and GAB (Guggenheim-Anderson-De Bore) models [25, 26], as depicted in Table 1, in the Microsoft Office Excel 2019 application. The regression coefficient ( $R^2$ ) was used to evaluate the goodness of fit of the two modes. Statistical parameters such as the correlation coefficient ( $R^2$ ), root mean square error (RMSE), and chi-square ( $\chi^2$ ) were used to evaluate the goodness of fit of the selected models.

**2.3. Drying of Sweet Potato Slices.** The sweet potato slices were dried using a cabinet drier (International Commercial Trades, Seoul, Korea, 136-120), which has different chambers for samples to be placed in trays (Figure 1). An anemometer was used to measure the air velocity as it was being blown over a heater by a fan. The dryer was turned on before placing the sample on the tray to achieve the desired drying temperature at an equilibrium state before commencing the drying experiments. The sample was subjected to three different temperatures (45, 55, and 62°C) at a constant air velocity of 0.6 m/sec. The mass change of samples during drying was recorded by comparing them with the initial moisture content to calculate the moisture ratio, which is required to analyze the drying kinetics of sweet potato slices. The thickness effect on drying kinetics was estimated using three different slice thicknesses (3, 5, and 7 mm), and the temperature effect on drying kinetics was estimated using two different thicknesses (3 and 5 mm). The loading densities were 10.82 kg/m<sup>2</sup> (single layer), 21.64 kg/m<sup>2</sup> (double layer), and 32.46 kg/m<sup>2</sup> (triple layer) for French cut and 9.72 kg/m<sup>2</sup> (single layer), 19.44 kg/m<sup>2</sup> (double layer), and 29.16 kg/m<sup>2</sup> (triple layer) for cubes to know the loading density of sweet potato slices on drying kinetics at 55°C. A schematic diagram of the sweet potato drying process is illustrated in Figure 2.

**2.4. Drying Kinetics and Mathematical Modeling.** The drying kinetics for sweet potato slices was determined on the basis of mass losses of potato slices. The moisture ratio

(MR) for the sweet potato slices was determined from the following equation:

$$MR = \frac{M_t - M_e}{M_0 - M_e}, \quad (1)$$

where  $M_t$ ,  $M_0$ , and  $M_e$  indicate the moisture contents at any time, the initial moisture content, and the equilibrium moisture content (kg water/kg dry matter), respectively, and  $t$  is the drying time (min).

In comparison to the values of  $M_t$  and  $M_0$ ,  $M_e$  has a relatively low value during long drying periods. So, the equation can be simplified as follows [28, 29]:

$$MR = \frac{M_t}{M_0}. \quad (2)$$

The drying data were fitted with six thin-layer drying models using nonlinear least square regression analysis to determine the best mathematical model for describing MR changes over drying time, which was widely used in previous studies [7, 30, 31]. Curve Expert Professional was used to perform statistical analyses on the experimental data (version 2.7.3, Hyams Development, Dallas, TX). Statistical parameters such as the correlation coefficient ( $R^2$ ), root mean square error (RMSE), and chi-square ( $\chi^2$ ) were used to evaluate the goodness of fit of the selected models. The highest correlation coefficient ( $R^2$ ), the lowest values of root mean square error (RMSE), and reduced chi-square ( $\chi^2$ ) were considered for the goodness of fit. These parameters were calculated using the following equations:

$$RMSE = \left[ \frac{\sum_{i=1}^N (MR_{exp,i} - MR_{pred,i})^2}{N} \right]^{1/2}, \quad (3)$$

$$\chi^2 = \frac{\sum_{i=1}^N (MR_{exp,i} - MR_{pred,i})^2}{N - Z},$$

where  $MR_{exp,i}$ ,  $MR_{pred,i}$ ,  $N$ , and  $Z$  are the  $i^{th}$  experimentally observed moisture ratio, the  $i^{th}$  predicted moisture ratio, the number of observations, and the number of constants.

**2.5. Computation of Effective Moisture Diffusivity.** It is presumed that food dehydration proceeds by a dilution method. Moisture diffuses to the surface during drying by a physical phenomenon known as diffusivity, which is explicable by Fick's diffusion equation [32]. Effective moisture diffusivity ( $D_{eff}$ ) of food products can be estimated using the "methods of slope" technique using Fick's second law of diffusion as follows:

$$\frac{\partial M}{\partial t} = D_{eff} \nabla^2 M, \quad (4)$$

where  $M$  stands for the moisture content (kg water/kg dry matter),  $t$  is the time (s),  $D_{eff}$  indicates the effective moisture diffusivity (m<sup>2</sup>/s), and  $\nabla$  is the mass transfer gradient.

TABLE 1: The moisture sorption isotherm models for sweet potato slices.

Sorption model	Mathematical equation	References
BET	$m_e = \frac{m_o C a_w}{(1 - a_w) + (C - 1)(1 - a_w) a_w}$	[27]
GAB	$m_e = \frac{m_o C K a_w}{(1 - K a_w) + (1 - K a_w + C K a_w)}$	[34]

The symbols  $C$  and  $K$  stand for the corresponding model's experimental constants. Other parameters  $m_e$ ,  $m_o$ , and  $a_w$  indicate the equilibrium moisture content, monolayer moisture content, and water activity, respectively.



FIGURE 1: Photographic view of the laboratory cabinet dryer used for sweet potato drying.

Assuming uniform moisture distribution, negligible temperature gradient within the sample being dried, negligible external resistance, negligible external mass transfer resistance, and constant diffusivity, the equation (Equation (4)) can be written as follows:

$$MR = \frac{8}{\pi^2} \sum_{n=0}^{\infty} \frac{1}{(2n+1)} \exp\left(-\frac{(2n+1)^2 \pi^2 D_{eff} t}{4L^2}\right), \quad (5)$$

where  $D_{eff}$  is the effective moisture diffusivity ( $m^2/s$ ),  $L$  is the half-thickness of the slab ( $m$ ), and  $n$  is the positive integer.

In the falling rate stage for long drying times, Equation (5) can be simplified to a limiting form of the diffusion equation as follows:

$$MR = \frac{8}{\pi^2} \exp\left(-\frac{\pi^2 D_{eff} t}{4L^2}\right). \quad (6)$$

Further, Equation (6) could be expressed into a straight-line equation in a logarithmic form as

$$\ln MR = \ln\left(\frac{8}{\pi^2}\right) - \left(\frac{\pi^2 D_{eff} t}{4L^2}\right) = \ln\left(\frac{8}{\pi^2}\right) - mt. \quad (7)$$

A plotting of  $\ln MR$  vs. drying time from Equation (7) resulted in the straight line with the following slope ( $m$ ) of

$$m = \frac{\pi^2 D_{eff}}{4L^2}, \quad (8)$$

where  $m$  is a drying rate constant ( $sec^{-1}$ ).

The experimental data were analyzed using Equation (7). The drying rate constant ( $m$ ) was obtained as the slope of the line by plotting moisture ratio (MR) against drying time ( $t$ ) plotting on a semilog coordinate, and the regression equations were developed as shown in Tables 2 and 3.

**2.6. Computation of Activation Energy.** The Arrhenius equation, in general, could be used to characterize the temperature dependency of effective moisture diffusivity as follows [33]:

$$D_{eff} = D_o \exp\left(-\frac{E_a}{R(T + 273.15)}\right), \quad (9)$$

where  $D_o$ ,  $E_a$ ,  $T$  and  $R$  represent the Arrhenius constant ( $m^2/s$ ), activation energy ( $kJ/mol$ ), temperature of air ( $^{\circ}C$ ), and universal gas constant ( $kJ/mol$ ). Equation (9) can be rearranged into the form of

$$\ln D_{eff} = \ln D_o - \frac{E_a}{R(T + 273.15)}. \quad (10)$$

The activation energy of diffusion of water was estimated from the slope ( $-E_a/R$ ) by plotting  $\ln D_{eff}$  against

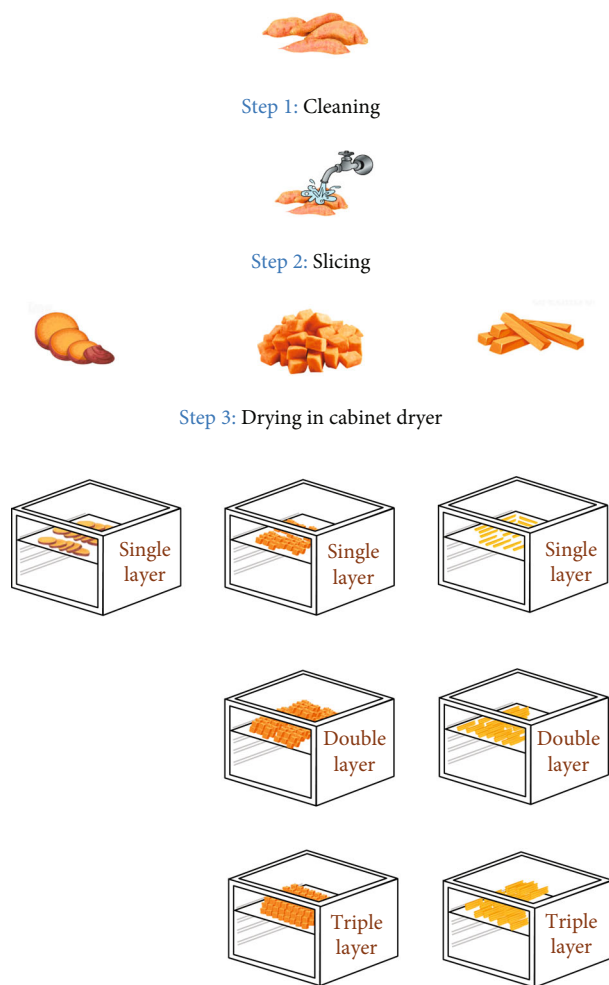


FIGURE 2: Schematic diagram of the sweet potato drying process.

TABLE 2: Effect of slice thickness (3, 5, and 7 mm) on drying rate constant.

Drying temperature (°C)	Sweet potato variety LSPS
45	$MR = 1.026e^{-0.31t}$ (for 3 mm; $t = \text{hr}$ )
	$MR = 0.971e^{-0.19t}$ (for 5 mm; $t = \text{hr}$ )
	$MR = 0.998e^{-0.16t}$ (for 7 mm; $t = \text{hr}$ )
55	$MR = 1.009e^{-0.32t}$ (for 3 mm; $t = \text{hr}$ )
	$MR = 0.963e^{-0.20t}$ (for 5 mm; $t = \text{hr}$ )
	$MR = 0.976e^{-0.16t}$ (for 7 mm; $t = \text{hr}$ )
62	$MR = 0.945e^{-0.29t}$ (for 3 mm; $t = \text{hr}$ )
	$MR = 0.941e^{-0.22t}$ (for 5 mm; $t = \text{hr}$ )
	$MR = 0.940e^{-0.17t}$ (for 7 mm; $t = \text{hr}$ )

inverse temperature ( $1/(T + 273.15)$ ) on linear coordinates. The linear regression procedure in Excel 2019 Professional performed linear regression analyses to fit the equation to the experimental data and determine the regression coefficient ( $R^2$ ).

TABLE 3: Effect of drying temperature (45, 55, and 62°C) on drying rate constant.

Thickness (mm)	Sweet potato variety LSPS
3	$MR = 0.990e^{-0.27t}$ (for 45°C; $t = \text{hr}$ )
	$MR = 0.974e^{-0.29t}$ (for 55°C; $t = \text{hr}$ )
	$MR = 0.945e^{-0.30t}$ (for 62°C; $t = \text{hr}$ )
5	$MR = 0.971e^{-0.19t}$ (for 45°C; $t = \text{hr}$ )
	$MR = 0.963e^{-0.20t}$ (for 55°C; $t = \text{hr}$ )
	$MR = 0.941e^{-0.22t}$ (for 62°C; $t = \text{hr}$ )

### 3. Result and Discussion

3.1. *Moisture Sorption Isotherm (MSI) and Mathematical Model Fitting.* The adsorption isotherms of the sweet potato variety named local sada (LSPS) (70.10% wb) at room temperature are shown in Figure 3. It demonstrated a typical type II sigmoidal sorption curve as a function of water activity ( $a_w$ ) based on the isotherms described by Brunauer [34]. The equilibrium moisture content (EMC) gradually increased with increasing  $a_w$  values from 0.1 to 0.7 and then sharply increased above the  $a_w$  value of 0.7. The sharp rise in EMC at  $a_w$  values higher than 0.7 is likely due to the sugar transitioning from a crystallized to an amorphous state [35]. Improved storage conditions, particularly a controlled humid environment, would be required better to comprehend the moisture absorption behavior of the sample. The lower part of the isotherms, especially below 0.6, shows microbial stability at lower humidity levels. Oh et al. [14] also reported a similar moisture isotherm for sweet potato.

Data from experimental adsorption isotherms were employed to fit a mathematical model. The monolayer moisture contents obtained using the BET and GAB models are presented in Table 4. The monolayer moisture is the moisture firmly attached to the food and is assumed to be the moisture content for the food material to be the most stable while being stored [36]. It is hypothesized that a product with a moisture content below the monolayer moisture content will exhibit a higher degree of stability according to chemical reactions that rely on solvation [37]. Our current study observed that the monolayer moisture content predicted by the GAB model was slightly higher than that predicted by the BET model. The monolayer moisture content ( $m_o$ ) estimated from the BET and GAB models was 5.917 g water/100 g solid and 6.481 g water/100 g solid, respectively. In a previous study, Sopade et al. [26] found the  $m_o$  of 4.82% and 4.66% from the BET and GAB models for a Nigerian sweet potato. The model with the highest  $R^2$ , the lowest  $\chi^2$ , and the lowest RMSE was considered the main criterion for choosing the best fitting the studied model to the experimental data. Based on these criteria, the GAB model was more fit to clarify the adsorption isotherm of LSPS at 30°C. The GAB model showed higher  $R^2$ , lower  $\chi^2$ , and RMSE compared to the BET model. However, in our study, the BET model was found to describe (good fit) the adsorption isotherms of LSPS accurately only in the range of water

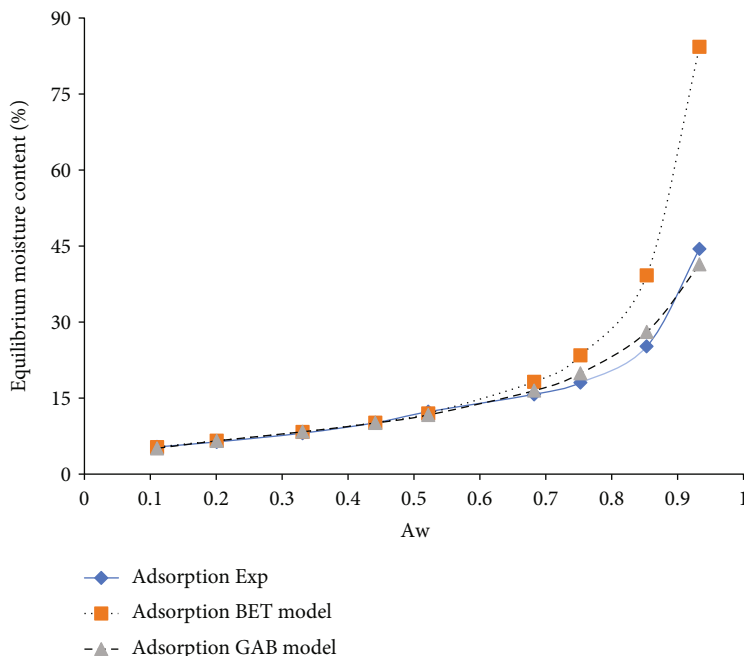


FIGURE 3: Experimental and predicted adsorption isotherm curve of LSPS at 30°C.

TABLE 4: Coefficients for the BET and GAB isotherms for LSPS.

Model constants, coefficient, and statistical parameters	Model	
	BET	GAB
$m_o$ (g water/100 g solid)	5.917	6.481
$C$	33.80	22.09
$K$	—	0.90803
$R^2$	0.8954	0.97850
RMSE	2.23	1.56978
$\chi^2$	35.64	3.16826

activity below 0.6. After which, an upward deflection was noticed. In contrast, the GAB model demonstrates a good fit across the entire range of water activity.

### 3.2. Drying Characteristics of Sweet Potato Slices

**3.2.1. Effect of Drying Temperature and Slice Thickness on Drying Time.** Figures 4(a)–4(c), depicting the moisture ratio vs. drying time, demonstrate the effect of constant drying temperature on the moisture ratio and drying time of the LSPS slices at 3, 5, and 7 mm thickness. It was observed that the MR decreased gradually with increasing drying time. At constant sample thickness, a rise in drying temperature accelerated the drying process. It was apparent that, for the 3 mm slice (Figure 4(a)), the drying time was shorter when the drying air temperature was 62°C as compared to 45 and 55°C. This was attributed to the increasing energy of water molecules as the temperature increased, and water molecules evaporated from the sample more rapidly. The findings demonstrated that drying time decreased with increasing drying temperature which corroborate with previous studies [30, 38].

The effect of slice thickness at various drying temperatures on moisture ratio with drying time is shown in Figures 5(a)–5(c). The figures show that the drying time increased noticeably as the slice thickness increased from 3 to 7 mm. Other investigations [39, 40] have shown that the thickness of the drying sample has a significant effect on the drying time which is possibly due to the water needs to travel more distance to reach the slice surface during the drying process. From Figure 5(a), it is evident that the 3 mm slice demonstrated a considerable decline in moisture ratio with increased drying time at a 45°C drying temperature. The drying temperatures of 55 and 65°C showed a similar decreasing trend of moisture ratio with drying time. The impact of temperature and slice thickness on the moisture ratio of our findings with regard to drying time was consistent with a previous study on Madeira bananas and Esmolfe apples [41].

**3.2.2. Effect of Slice Thickness on Drying Kinetics.** The impact of thickness on the drying rate constant of LSPS at 45, 55, and 62°C is summarized in Table 2. Fick's second law of diffusion was used to estimate the drying rate constant from the slope of  $\ln MR$  versus drying time (Equation (7)). The obtained equation suggests that drying rate constants decreased with increasing slice thickness for all given temperatures. For the temperature of 45°C, the drying rate constant was 0.31 h<sup>-1</sup> for 3 mm thickness slices, but that value decreased to 0.19 h<sup>-1</sup> and 0.16 h<sup>-1</sup> for 5 mm and 7 mm thickness slices, respectively. The sample drying at 55 and 62°C also exhibited the same downward trend of constant drying rate, as shown in Table 2. This may be due to a decrease in drying rate to a particular moisture ratio with an increase in sample thickness at a constant temperature, which led to a decline in the drying rate constant [21]. This

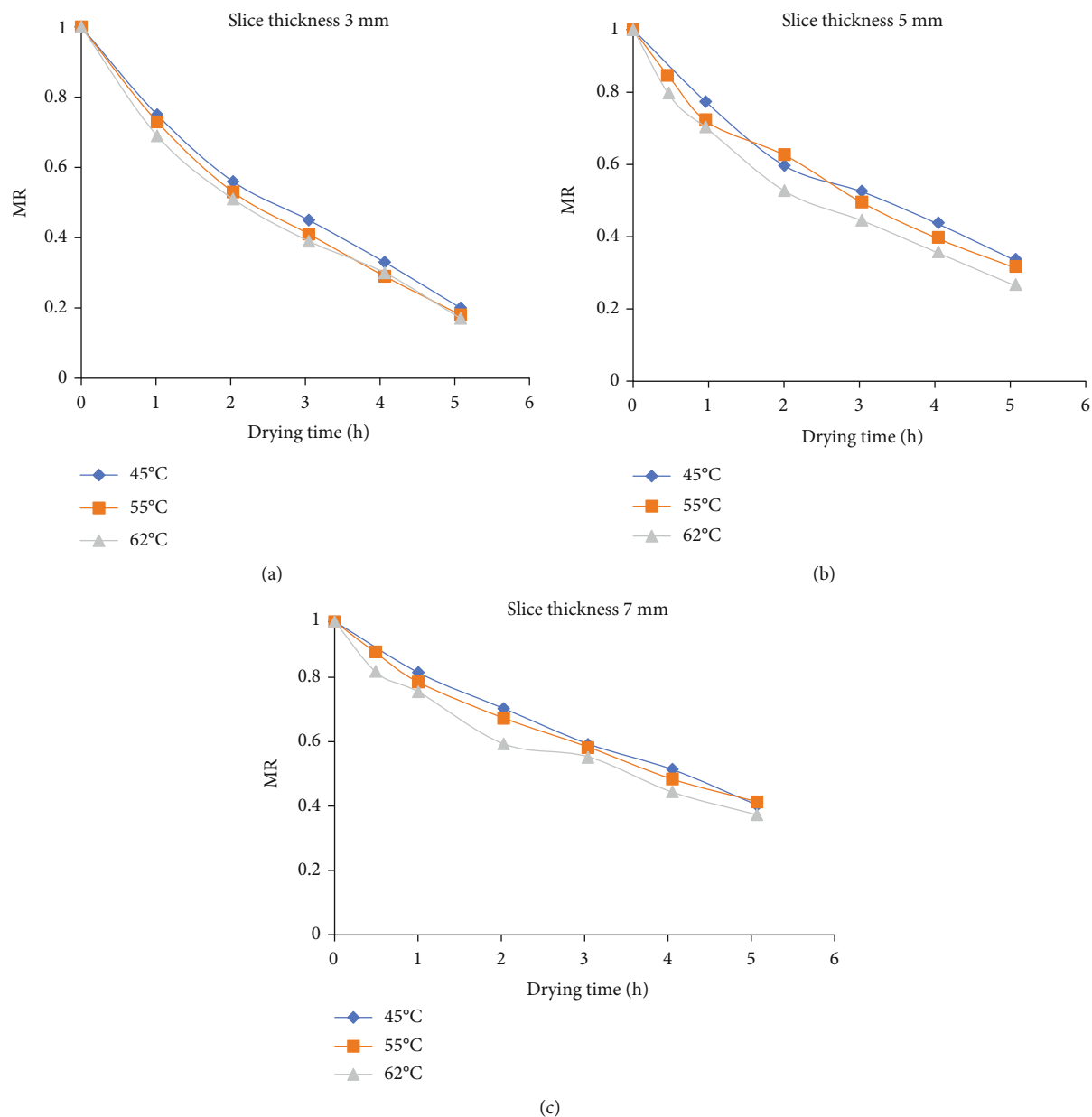


FIGURE 4: (a–c) Effect of temperature on the moisture ratio (MR) of LSPS slices at any drying time.

phenomenon also might possibly be due to the larger distance traveled by moisture reaching the product's surface. An increase in drying rate constant with thickness has also been reported by Rahman et al. [21] for 4, 6, and 8 mm banana slices at temperatures 45, 55, and 65°C.

**3.2.3. Effects of Temperature on Drying Kinetics.** The effect of drying temperatures on the drying rate constant of sweet potato slices at each of the two sample thicknesses (3 and 5 mm) is summarized in Table 3. The drying rate constant for constant slice thicknesses was found to be increased with increasing drying temperature, as reported in the previous study [42]. The increase of the drying rate constant at the higher temperature is possibly due to the faster evaporation of water molecules from the sample at higher temperatures,

which was caused by the greater energy of the water molecule [11]. The drying rate constant for 3 mm slices was higher than that of 5 mm slices. With an increase in temperature from 45°C to 62°C, the drying rate constant for 3 mm and 5 mm slices increased from  $0.27 \text{ h}^{-1}$  to  $0.30 \text{ h}^{-1}$  and from  $0.19 \text{ h}^{-1}$  to  $0.22 \text{ h}^{-1}$ , respectively. Like our study, a consistent increasing trend of drying rate constant corresponding to increased drying temperature has also been reported for wheat [43] and banana [21] drying.

**3.2.4. Mathematical Modeling of Thin-Layer Drying of LSPS Slices.** The drying of LSPS slices at various temperatures was described using five thin-layer drying models, along with the Lewis, Henderson and Pabis, logarithmic, Page, and Wang and Singh models. The best drying model was

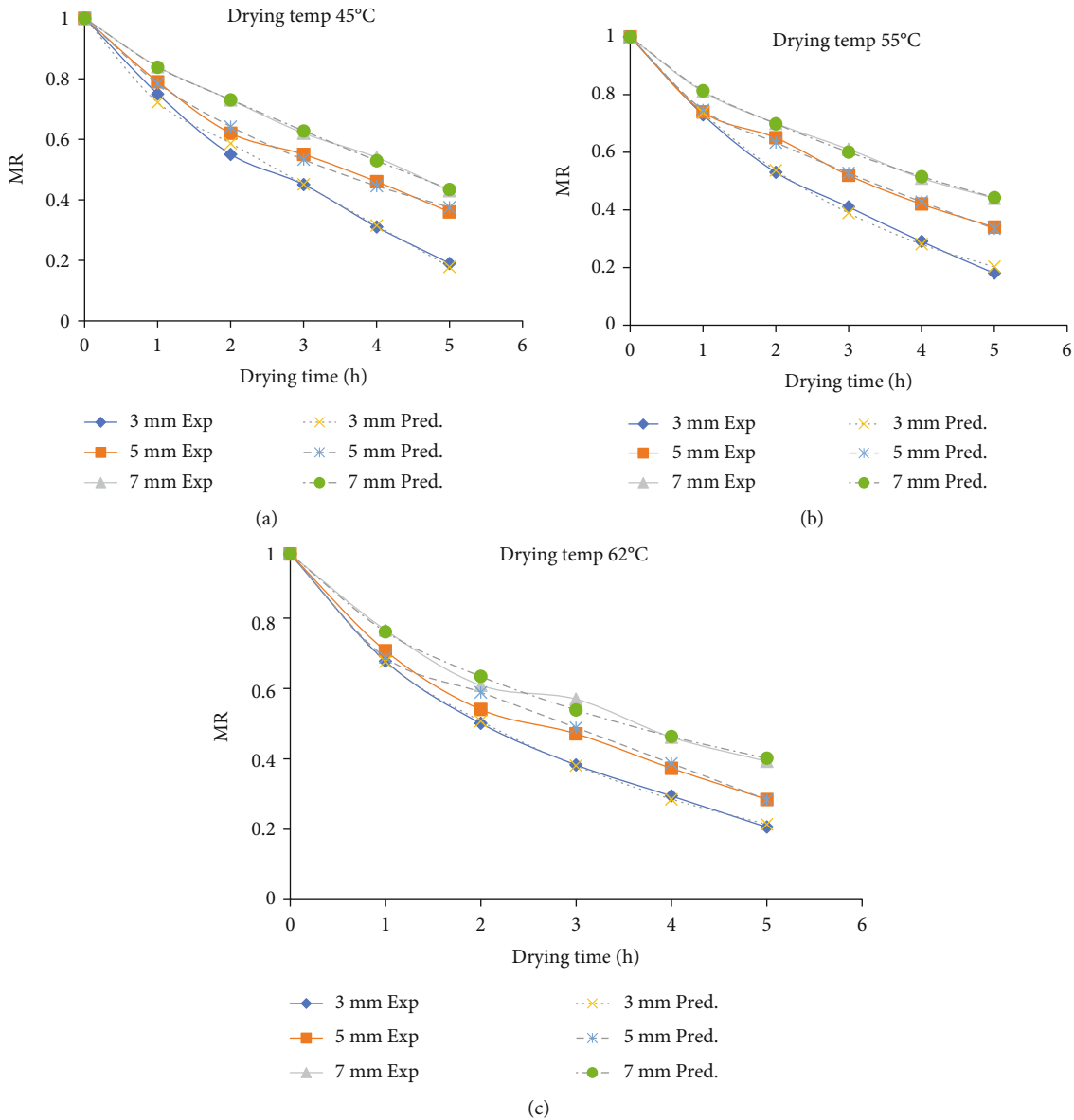


FIGURE 5: (a–c) Effect of slice thickness on the moisture ratio (MR) of the LSPS slices at drying temperatures of 45, 55, and 62°C: (a) experimental data with logarithmic model, (b) experimental data with logarithmic model, and (c) experimental data with the Page model.

selected based on models with the highest correlation coefficient ( $R^2$ ), the lowest values of root mean square error (RMSE), and reduced chi-square ( $\chi^2$ ), which shows that the investigated model closely fits the experimental data. The findings of the regression analysis that was carried out to fit the experimental data are presented in Table 5. According to these standards, the logarithmic model at 45°C and 55°C and the Page model at 62°C were found to be the best fittest models to clarify the drying curve of LSPS slices (Table 5). Previous studies also found the logarithmic model [23] at temperatures of 50–70°C and the Page model [22] at temperatures of 50 and 80°C best fit for experimental drying data for sweet potato slices. The correlation between the predicted MR and the experimental MR of the chosen models at selected drying temperatures is shown in Figures 6(a)–6(e) to

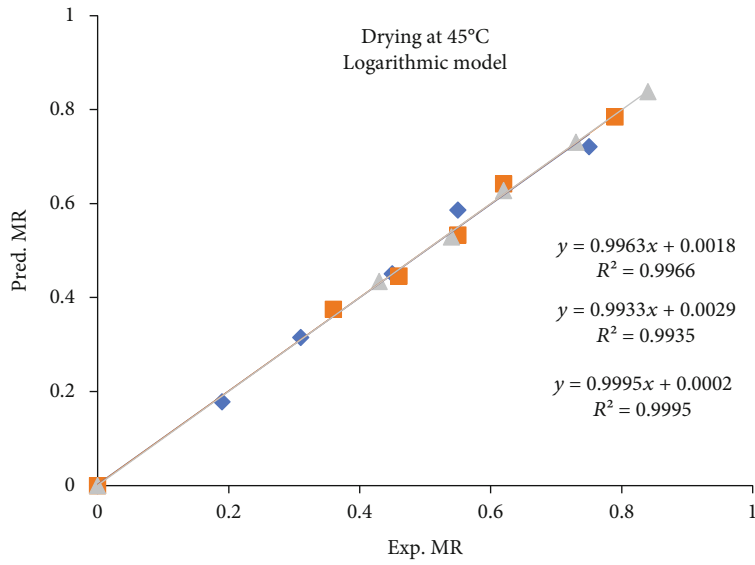
validate the best model. It is observed that the  $R^2$  values for the best models were greater than 99, which is near 1 and indicates that the data were tightly clustered around a 45° straight line. So, our predicted logarithmic model at 45–55°C and Page model at 62°C are suitable to describe the drying characteristics of sweet potato slices.

**3.2.5. Effective Moisture Diffusivity.** The values of effective moisture diffusivity ( $D_{eff}$ ) were obtained from different drying conditions using Equation (8) and summarized in Table 6. The  $D_{eff}$  values of the LSPS sample appeared to be affected by drying temperature and slice thickness. The  $D_{eff}$  values were found in the range of  $7.60 \times 10^{-11}$  to  $1.34 \times 10^{-10}$  m<sup>2</sup>/s for 3 mm and 5 mm thick slices at the temperature of 45 to 62°C with higher  $R^2$  values ranging from

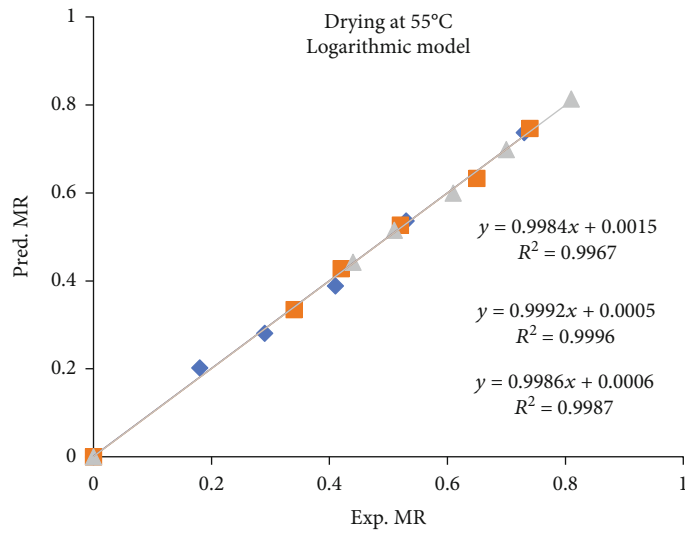


TABLE 5: Statistical results of different drying models and their constants and regression coefficients at different temperatures and slice thickness.

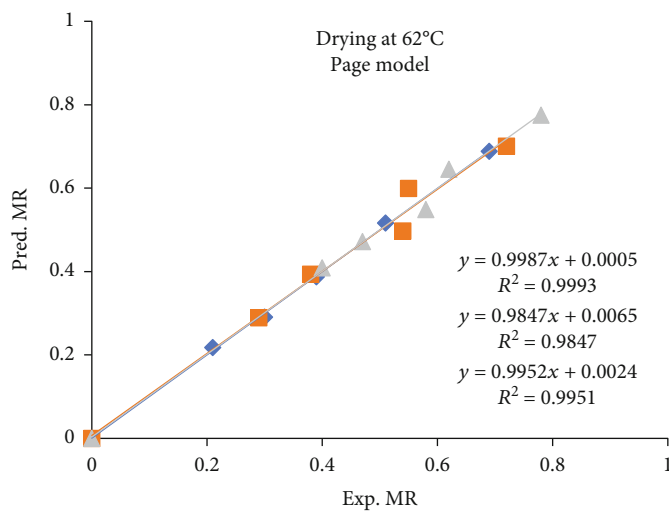
Model	Drying temp (°C) with slice thickness	$k$	Model constants				$R^2$	RMSE	$\chi^2$
			$a$	$b$	$c$	$n$			
Lewis	45°C, 3 mm	0.294					0.98426	0.02428	0.00074
	45°C, 5 mm	0.207					0.97255	0.32976	0.13592
	45°C, 7 mm	0.161					0.99339	0.01163	0.00291
	55°C, 3 mm	0.315					0.99326	0.01569	0.00031
	55°C, 5 mm	0.222					0.96249	0.02830	0.00100
	55°C, 7 mm	0.170					0.98240	0.01749	0.00038
	62°C, 3 mm	0.321					0.98432	0.02098	0.00055
	62°C, 5 mm	0.249					0.89736	0.04772	0.00285
	62°C, 7 mm	0.196					0.92686	0.03539	0.00157
Henderson and Pabis	45°C, 3 mm	0.303	1.024				0.98519	0.02354	0.00092
	45°C, 5 mm	0.186	0.939				0.98770	0.01619	0.00044
	45°C, 7 mm	0.160	0.995				0.99353	0.01150	0.00022
	55°C, 3 mm	0.318	1.009				0.99340	0.01553	0.00040
	55°C, 5 mm	0.192	0.917				0.98969	0.01483	0.00037
	55°C, 7 mm	0.152	0.947				0.99473	0.00957	0.00023
	62°C, 3 mm	0.287	0.917				0.99783	0.00780	0.00010
	62°C, 5 mm	0.206	0.883				0.94584	0.03466	0.00225
	62°C, 7 mm	0.162	0.903				0.97835	0.01925	0.00062
Logarithmic	45°C, 3 mm	-0.005	-29.475		30.331		0.98763	0.02153	0.00116
	45°C, 5 mm	0.192	0.924		0.017		0.98828	0.01580	0.00042
	45°C, 7 mm	0.044	2.622		-1.671		0.99801	0.00638	0.00010
	55°C, 3 mm	-0.003	-41.200		42.028		0.99383	0.01501	0.00038
	55°C, 5 mm	0.065	1.922		-1.054		0.99566	0.00962	0.00023
	55°C, 7 mm	-0.004	-22.016		22.907		0.99829	0.00545	0.00005
	62°C, 3 mm	-0.002	-63.716		64.487		0.97468	0.02667	0.00178
	62°C, 5 mm	-0.012	-8.204		9.004		0.93792	0.03711	0.00230
	62°C, 7 mm	0.194	0.822		0.092		0.97865	0.01912	0.00091
Page	45°C, 3 mm	0.27441				1.063	0.98663	0.02237	0.00083
	45°C, 5 mm	0.24281				0.867	0.98771	0.11806	0.03485
	45°C, 7 mm	0.15991				1.007	0.99342	0.01160	0.00022
	55°C, 3 mm	0.30476				1.030	0.98357	0.02449	0.00150
	55°C, 5 mm	0.26354				0.853	0.98207	0.01956	0.00064
	55°C, 7 mm	0.19771				0.875	0.99578	0.00856	0.00012
	62°C, 3 mm	0.36523				0.878	0.99856	0.00637	0.00007
	62°C, 5 mm	0.31400				0.800	0.95630	0.03114	0.00200
	62°C, 7 mm	0.25473				0.780	0.97959	0.01869	0.00058
Wang and Singh	45°C, 3 mm		-0.246	0.017			0.98572	0.02312	0.00089
	45°C, 5 mm		-0.209	0.017			0.97396	0.02355	0.00092
	45°C, 7 mm		-0.150	0.008			0.99268	0.01224	0.00025
	55°C, 3 mm		-0.269	0.022			0.98906	0.01999	0.00067
	55°C, 5 mm		-0.219	0.018			0.96028	0.02912	0.00141
	55°C, 7 mm		-0.175	0.013			0.98611	0.01554	0.00040
	62°C, 3 mm		-0.296	0.028			0.97363	0.02721	0.00123
	62°C, 5 mm		-0.244	0.021			0.88577	0.05034	0.00422
	62°C, 7 mm		-0.211	0.019			0.95108	0.02894	0.00140



(a)

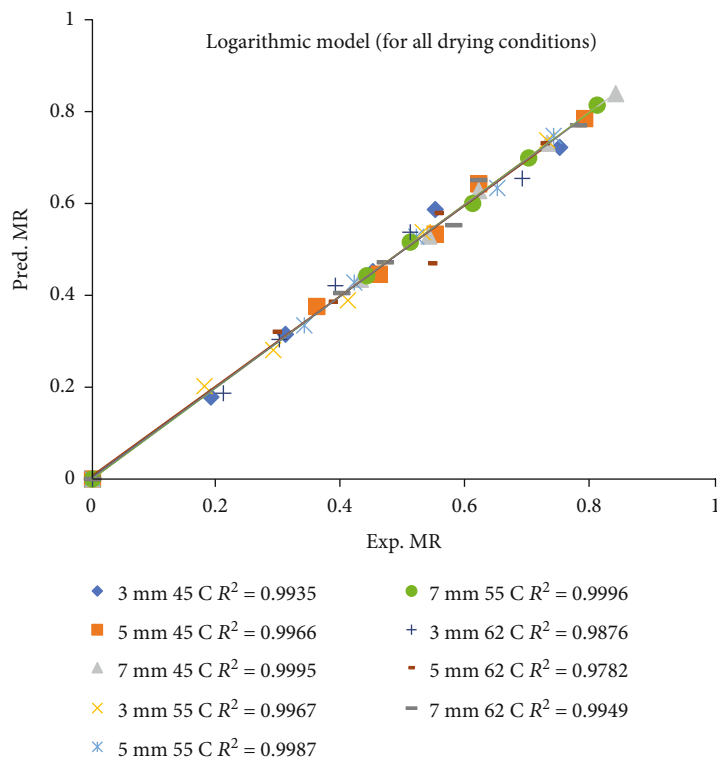


(b)

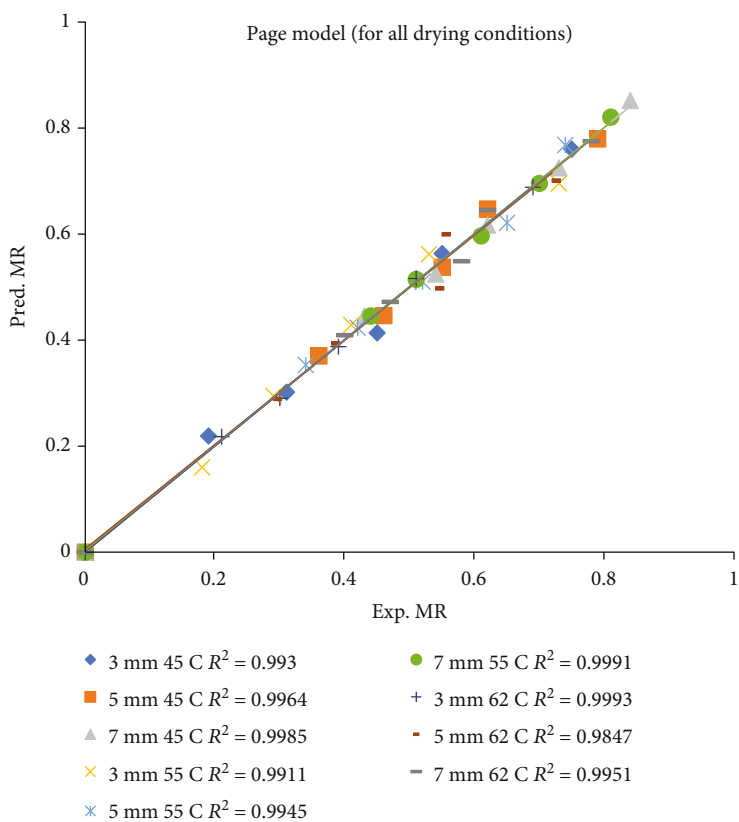


(c)

FIGURE 6: Continued.



(d)



(e)

FIGURE 6: (a-e) Correlation between predicted moisture ratio (Pred. MR) and experimental moisture ratio (Exp. MR) representing the validation of the models at 45-62°C drying temperature.

TABLE 6: Effective moisture diffusivity of sweet potato slices.

Sweet potato	Temp (°C)	Sample thickness (mm)	Effective moisture diffusivity (m <sup>2</sup> /s)	Standard deviation (R <sup>2</sup> )
LSPS	45	3	$6.85 \times 10^{-11}$	0.9955
		5	$1.34 \times 10^{-10}$	0.9921
	55	3	$7.35 \times 10^{-11}$	0.9966
		5	$1.41 \times 10^{-10}$	0.9900
	62	3	$7.60 \times 10^{-11}$	0.9906
		5	$1.55 \times 10^{-10}$	0.9682

TABLE 7: The activation energy values for sweet potato slices.

Sweet potato	Sample thickness (mm)	Activation energy value (kJ/mol)	Standard deviation (R <sup>2</sup> )
LSPS	3	5.55	0.9924
	5	7.39	0.9196

TABLE 8: Effect of sample loading density (LD) on drying rate constant at 55°C.

Sweet potato	Sample shape	
	French cut	Cube cut
LSPS	MR = $1.093e^{-0.19x}$ for LD 10.82 kg/m <sup>2</sup>	MR = $0.998e^{-0.18x}$ for LD 9.72 kg/m <sup>2</sup>
	MR = $1.073e^{-0.12x}$ for LD 21.64 kg/m <sup>2</sup>	MR = $1.025e^{-0.13x}$ for LD 19.44 kg/m <sup>2</sup>
	MR = $1.042e^{-0.07x}$ for LD 32.46 kg/m <sup>2</sup>	MR = $1.013e^{-0.07x}$ for LD 29.16 kg/m <sup>2</sup>

0.9682 to 0.9966. High  $R^2$  values indicated a well-fitted empirical relationship between the values of  $\ln(MR)$  and drying time, which describes the moisture diffusivity well. The  $D_{\text{eff}}$  values of this experiment fall within the standard limits of  $10^{-12}$  to  $10^{-8}$  m<sup>2</sup>/s for drying food products [44]. In our study, LSPS experienced an increase of  $D_{\text{eff}}$  with increasing the drying temperature probably due to an increase in heating energy at the higher temperature, which would enhance the rapid migration of water particles to the sample surface, resulting in higher moisture diffusivity [45], due to the fact that higher temperatures increase a sample's internal vapor pressure, which in turn causes water molecules to quickly migrate to the sample's surface and increase moisture diffusivity [46]. A similar observation for  $D_{\text{eff}}$  values has been reported by Sairam et al. [47] for air-drying papaya slices and by Doymaz [29] for air-drying white button mushroom slices. Furthermore, the results for  $D_{\text{eff}}$  in the current study were supported by previous research experiments conducted for drying sweet potato slices, and they found the  $D_{\text{eff}}$  of  $1.32 \times 10^{-11}$  to  $1.75 \times 10^{-10}$  m<sup>2</sup>/s at the temperature between 50 and 70°C [23].

**3.2.6. Activation Energy.** The activation energy ( $E_a$ ) revealed the sensitivity to temperature and the energy required to induce moisture diffusion inside the slice. The values of activation energy of sliced sweet potato have shown in Table 7. It was found that the activation energy values increased with increasing slice thickness as stated in previous studies [24, 47]. The  $E_a$  was found to be 5.55 and 7.39 kJ/mol for 3 mm and 5 mm slices, respectively, within the range of air temper-

ature of 45–62°C. These findings revealed that 3 mm slices required lower activation energy than 5 mm. It indicates that it was easier to introduce the water release process in the 3 mm than in the 5 mm slice during the drying process. Our findings of  $E_a$  were lower compared to Dinrifo [7], who estimated that the  $E_a$  of a Nigerian variety was 17.5 kJ/mol. This is likely owing to the fact that the activation energy ( $E_a$ ) of products is highly related to their composition, tissue structures, and specific surface area, along with their variety, maturation stage, and even pretreatments [48]. Furthermore, an increase in  $E_a$  values with increasing pumpkin sample thickness has been observed by Limpiboon [11]. A similar trend was observed in our investigation.

**3.2.7. Effect of Tray Loading Density and Shape of Sample on Drying Kinetics.** The sweet potato slices (French cut and cube cut) were loaded in a mechanical dryer at three different densities to measure the effects of loading density on the drying rate constant at 55°C. The drying rate constant for the French cut and cube cut samples decreased as tray loading density increased from a thin to a triple layer (Table 8). The drying rate constant of the French cut LSPS reduced by 63% from  $0.19 \text{ h}^{-1}$  (thin layer) to  $0.07 \text{ h}^{-1}$  (triple layer), while cube cut LSPS lowered by 61% from  $0.18 \text{ h}^{-1}$  (thin layer) to  $0.07 \text{ h}^{-1}$  (triple layer). The shape of sweet potato slices (French cut and cube cut) exhibited an almost similar effect on the drying rate constant. The current findings were supported by Hosain et al. [43], who reported that the drying rate constantly decreased with the increased loading density of wheat. In contrast, Paul and Martynenko [49] did not find any effect

of load density on the drying rate constant during apple drying in an electrohydrodynamic (EHD) dryer.

#### 4. Conclusion

This research examined the moisture sorption behavior and the influence of slice thickness, drying temperature, and loading density on the drying characteristics with thin-layer kinetic models, moisture diffusivity, and activation energy of sweet potato slices. The GAB model was more appropriate than the BET model for describing the adsorption isotherm. Increased slice thickness and tray loading density markedly reduced the drying rate constant. Six thin-layer models were considered to anticipate the drying process of an LSPS slice, whereas the logarithmic and Page models confirmed the goodness of fit for the majority of the data indicated by the highest  $R^2$  and the lowest RMSE and  $\chi^2$  values. Effective moisture diffusivity increased with increasing temperature and thickness, with values ranging between  $7.10 \times 10^{-11}$  and  $1.55 \times 10^{-10}$  m<sup>2</sup>/s over the temperature range studied. The activation energy values rose as slice thickness grew. Examining the effects of various factors, such as temperature, slice thickness, and loading densities on the nutritional qualities, the properties of dried material of sweet potato slices are a further direction.

#### Data Availability

All data are available in the manuscript.

#### Conflicts of Interest

There is no conflict of interest to declare.

#### Acknowledgments

The authors are thankful to Dr. Mohammad Rezaul Islam Shishir (postdoctoral researcher of Shenzhen University, Shenzhen, Guangdong, China) and Faridunnabi Nayem (researcher, Department of Food Technology, Chulalongkorn University, Thailand) for their cooperation.

#### References

- [1] R. O. Mwanga, M. I. Andrade, E. E. Carey, J. W. Low, G. C. Yenchu, and W. J. Grüneberg, "Sweetpotato (*Ipomoea batatas* L.)," in *Genetic Improvement of Tropical Crops*, pp. 181–218, Springer, Cham, 2017.
- [2] S. A. Tadda, X. Kui, H. Yang et al., "The response of vegetable sweet potato (*Ipomoea batatas* Lam) nodes to different concentrations of encapsulation agent and MS salts," *Agronomy*, vol. 12, no. 1, p. 19, 2021.
- [3] OECD and Food and Agriculture Organization of the United Nations, "OECD-FAO Agricultural Outlook 2022-2031," OECD Publishing, Paris, 2022.
- [4] APAC Statista, "Sweet potato production volume in the Asia-Pacific region in 2020, by country: (in 1,000 metric tons)," 2019, <https://www.statista.com/statistics/681959/asia-pacific-sweet-potato-production-by-country/>.
- [5] BBS, "Bangladesh Bureau of Statistics," in *Statistics and Information Division*, Ministry of Planning, Dhaka, Bangladesh, 2020.
- [6] M. M. Hossain, M. A. Rahim, H. N. Moutosi, and L. Das, "Evaluation of the growth, storage root yield, proximate composition, and mineral content of colored sweet potato genotypes," *Journal of Agriculture and Food Research*, vol. 8, article 100289, 2022.
- [7] R. R. Dinrifo, "Effects of pre-treatments on drying kinetics of sweet potato slices," *Agricultural Engineering International: CIGR Journal*, vol. 14, no. 3, pp. 136–145, 2012.
- [8] B. Dereje, A. Girma, D. Mamo, and T. Chalchisa, "Functional properties of sweet potato flour and its role in product development: a review," *International Journal of Food Properties*, vol. 23, no. 1, pp. 1639–1662, 2020.
- [9] R. Guine, "The drying of foods and its effect on the physical-chemical, sensorial and nutritional properties," *ETP International Journal of Food Engineering*, vol. 4, no. 2, pp. 93–100, 2018.
- [10] K. J. Bradford, P. Dahal, J. van Asbrouck et al., "The dry chain: reducing postharvest losses and improving food safety in humid climates," *Trends in Food Science and Technology*, vol. 71, pp. 84–93, 2018.
- [11] K. Limpiboon, "Effects of temperature and slice thickness on drying kinetics of pumpkin slices," *Walailak Journal of Science and Technology (WJST)*, vol. 8, no. 2, pp. 159–166, 2011.
- [12] M. Maskan, "Microwave/air and microwave finish drying of banana," *Journal of Food Engineering*, vol. 44, no. 2, pp. 71–78, 2000.
- [13] R. J. Mongi, "Physicochemical properties, microbial loads and shelf life prediction of solar dried mango (*Mangifera indica*) and pineapple (*Ananas comosus*) in Tanzania," *Journal of Agriculture and Food Research*, vol. 11, article 100522, 2023.
- [14] S. Oh, E.-J. Lee, and G.-P. Hong, "Quality characteristics and moisture sorption isotherm of three varieties of dried sweet potato manufactured by hot air semi-drying followed by hot-pressing," *LWT-Food Science and Technology*, vol. 94, pp. 73–78, 2018.
- [15] S. Ouertani, M. Simo-Tagne, and R. Rémond, "Sorption isotherms and moisture transfer properties of seven Central Africa hardwood species," *Wood Material Science & Engineering*, vol. 18, no. 2, pp. 507–516, 2023.
- [16] M. Simo-Tagne, L. Bennamoun, A. Léonard, and Y. Rogaume, "Determination and modeling of the isotherms of adsorption/desorption and thermodynamic properties of obeche and lotofa using Nelson's sorption model," *Heat and Mass Transfer*, vol. 55, no. 8, pp. 2185–2197, 2019.
- [17] M. Simo-Tagne, R. Rémond, Y. Rogaume, A. Zoulalian, and B. Bonoma, "Sorption behavior of four tropical woods using a dynamic vapor sorption standard analysis system," *Maderas. Ciencia y tecnología*, vol. 18, no. 3, pp. 403–412, 2016.
- [18] M. Simo-Tagne, R. Rémond, Y. Rogaume, A. Zoulalian, and P. Perré, "Characterization of sorption behavior and mass transfer properties of four Central Africa tropical woods: ayous, sapele, frake, lotofa," *Maderas. Ciencia y tecnología*, vol. 18, no. 1, pp. 207–226, 2016.
- [19] S. Yasmin, M. Hasan, M. Sohany, and M. S. H. Sarker, "Drying kinetics and quality aspects of bitter melon (*Momordica charantia*) dried in a novel cabinet dryer," *Food Research*, vol. 6, no. 4, pp. 180–188, 2022.

- [20] S. Yang, T. Liu, N. Fu, J. Xiao, A. Putranto, and X. D. Chen, "Convective drying of highly shrinkable vegetables: new method on obtaining the parameters of the reaction engineering approach (REA) framework," *Journal of Food Engineering*, vol. 305, article 110613, 2021.
- [21] M. H. Rahman, M. W. Ahmed, and M. N. Islam, "Drying kinetics and sorption behavior of two varieties banana (Sagor and Sabri) of Bangladesh," *SAARC Journal of Agriculture*, vol. 16, no. 2, pp. 181–193, 2019.
- [22] A. S. Olawale and S. O. Omole, "Thin layer drying models for sweet potato in tray dryer," *Agricultural Engineering International: CIGR Journal*, vol. 14, no. 2, pp. 131–137, 2012.
- [23] İ. Doymaz, "Thin-layer drying characteristics of sweet potato slices and mathematical modelling," *Heat and Mass Transfer*, vol. 47, no. 3, pp. 277–285, 2011.
- [24] N. J. Singh and R. K. Pandey, "Convective air drying characteristics of sweet potato cube (*Ipomoea batatas* L.)," *Food and Bioproducts Processing*, vol. 90, no. 2, pp. 317–322, 2012.
- [25] M. S. Alamri, A. A. Mohamed, S. Hussain, M. A. Ibraheem, A. Qasem, and A. Akram, "Determination of moisture sorption isotherm of crosslinked millet flour and oxirane using GAB and BET," *Journal of Chemistry*, vol. 2018, Article ID 2369762, 8 pages, 2018.
- [26] P. A. Sopade, E. S. A. Ajisegiri, O. Chukwu, and A. B. Abass, "Moisture-sorption isotherms of Irish and sweet potatoes," *Journal of Food Process Engineering*, vol. 33, no. 3, pp. 385–397, 2010.
- [27] M. Saberi and P. Rouhi, "Extension of the Brunauer-Emmett-Teller (BET) model for sorption of gas mixtures on the solid substances," *Fluid Phase Equilibria*, vol. 534, p. 112968, 2021.
- [28] A. Balbay and Ö. Şahin, "Microwave drying kinetics of a thin-layer liquorice root," *Drying Technology*, vol. 30, no. 8, pp. 859–864, 2012.
- [29] I. Doymaz, "Drying kinetics and rehydration characteristics of convective hot-air dried white button mushroom slices," *Journal of Chemistry*, vol. 2014, Article ID 453175, 8 pages, 2014.
- [30] M. M. Kamal, M. R. Ali, M. R. I. Shishir, and S. C. Mondal, "Thin-layer drying kinetics of yam slices, physicochemical, and functional attributes of yam flour," *Journal of Food Process Engineering*, vol. 43, no. 8, article e13448, 2020.
- [31] Y. Wang, X. Li, X. Chen et al., "Effects of hot air and microwave-assisted drying on drying kinetics, physicochemical properties, and energy consumption of chrysanthemum," *Chemical Engineering and Processing: Process Intensification*, vol. 129, pp. 84–94, 2018.
- [32] P. Perre, "The proper use of mass diffusion equation in drying modelling: from simple configurations to non-fickian behaviours," in *19th International Drying Symposium IDS'2014*, Lyon, France, 2014.
- [33] S. Mghazli, M. Ouhammou, N. Hidar, L. Lahnine, A. Idlimam, and M. Mahrouz, "Drying characteristics and kinetics solar drying of Moroccan rosemary leaves," *Renewable Energy*, vol. 108, pp. 303–310, 2017.
- [34] R. D. Andrade, R. Lemus, and C. E. Perez, "Models of sorption isotherms for food: uses and limitations," *Vitae*, vol. 18, no. 3, pp. 325–334, 2011.
- [35] S. Thalerngnawachart and K. Duangmal, "Influence of humectants on the drying kinetics, water mobility, and moisture sorption isotherm of osmosed air-dried papaya," *Drying Technology*, vol. 34, no. 5, pp. 574–583, 2016.
- [36] B. D. Igbabul, C. C. Ariaahu, and E. U. Umeh, "Moisture adsorption isotherms of African arrowroot lily (*Tacca involu-crata*) tuber mash as influenced by blanching and natural fermentation," *Journal of Food Research*, vol. 2, no. 3, p. 79, 2013.
- [37] R. B. K. Anandito, L. Purnamayati, and H. Sodik, "Shelf-life determination of fish koya using critical moisture content approach: shelf-life determination of fish koya using critical moisture content approach," *Proceedings of the Pakistan Academy of Sciences: B. Life and Environmental Sciences*, vol. 54, no. 3, pp. 201–206, 2017.
- [38] N. Jiang, J. Ma, R. Ma et al., "Effect of slice thickness and hot-air temperature on the kinetics of hot-air drying of crabapple slices," *Food Science and Technology*, vol. 43, 2023.
- [39] S. Raut, R. Md Saleh, P. Kirchhofer, B. Kulig, O. Hensel, and B. Sturm, "Investigating the effect of different drying strategies on the quality parameters of *Daucus carota* L. using dynamic process control and measurement techniques," *Food and Bio-process Technology*, vol. 14, no. 6, pp. 1067–1088, 2021.
- [40] K. Vivek, K. V. Subbarao, and B. Srivastava, "Effect of thin-layer drying on the quality parameters of persimmon slices," *International Journal of Fruit Science*, vol. 21, no. 1, pp. 587–598, 2021.
- [41] M. C. Pinheiro, R. O. Madaleno, and L. M. Castro, "Drying kinetics of two fruits Portuguese cultivars (*Bravo de Esmolfe* apple and Madeira banana): An experimental study," *Heliyon*, vol. 8, no. 4, article e09341, 2022.
- [42] M. C. Ndukwu, "Effect of drying temperature and drying air velocity on the drying rate and drying constant of cocoa bean," *Agricultural Engineering International: CIGR Journal*, vol. 11, 2009.
- [43] M. Hosain, R. Haque, M. N. Islam, H. Khatun, and M. Shams-Ud-Din, "Effect of temperature and loading density on drying kinetics of wheat," *Journal of Experimental Biology and Agricultural Sciences*, vol. 4, no. 2, pp. 210–217, 2016.
- [44] T. Y. Tunde-Akintunde and A. A. Afon, "Modelling of hot-air drying of pretreated cassava chips," *Agricultural Engineering International: the CIGR Ejournal*, vol. 1493, 2009.
- [45] H.-W. Xiao, C.-L. Pang, L.-H. Wang, J.-W. Bai, W.-X. Yang, and Z.-J. Gao, "Drying kinetics and quality of Monukka seedless grapes dried in an air-impingement jet dryer," *Biosystems Engineering*, vol. 105, no. 2, pp. 233–240, 2010.
- [46] D. Zhao, J. Wei, J. Hao et al., "Effect of sodium carbonate solution pretreatment on drying kinetics, antioxidant capacity changes, and final quality of wolfberry (*Lycium barbarum*) during drying," *Lebensmittel-Wissenschaft & Technologie*, vol. 99, pp. 254–261, 2019.
- [47] N. Sairam, M. N. Kumar, L. Edukondalu, and G. Y. Kumar, "Effect of slice thickness on drying kinetics of papaya using food dehydrator," *International Journal of Agriculture, Environment and Biotechnology*, vol. 10, no. 6, pp. 749–756, 2017.
- [48] D. Wang, J. W. Dai, H. Y. Ju et al., "Drying kinetics of American ginseng slices in thin-layer air impingement dryer," *International Journal of Food Engineering*, vol. 11, no. 5, pp. 701–711, 2015.
- [49] A. Paul and A. Martynenko, "The effect of material thickness, load density, external airflow, and relative humidity on the drying efficiency and quality of EHD-dried apples," *Food*, vol. 11, no. 18, p. 2765, 2022.